Published in final edited form as:
Cell Stem Cell. 2009 April 3; 4(4): 336–347. doi:10.1016/j.stem.2009.02.015.

Mouse Fibroblasts Lacking RB1 Function Form Spheres and Undergo Reprogramming to a Cancer Stem Cell Phenotype

Yongqing Liu[1,2], **Brian Clem**[1], **Ewa K. Zuba-Surma**[3], **Shahenda El-Naggar**[1,2], **Sucheta Telang**[1], **Alfred B. Jenson**[1], **Yali Wang**[2], **Hui Shao**[2], **Mariusz Z. Ratajczak**[3], **Jason Chesney**[1], and **Douglas C. Dean**[1,2,4,*]

[1]Molecular Targets Program, Brown Cancer Center, University of Louisville Health Sciences Center, Louisville, KY 40202, USA

[2]Department of Ophthalmology and Visual Sciences, University of Louisville Health Sciences Center, Louisville, KY 40202, USA

[3]Stem Cell Biology Program, Brown Cancer Center, University of Louisville Health Sciences Center, Louisville, KY 40202, USA

[4]Department of Biochemistry and Molecular Biology, University of Louisville Health Sciences Center, Louisville, KY 40202, USA

SUMMARY

Activation of the RB1 pathway triggers the cell-cycle arrest that mediates cell-cell contact inhibition. Accordingly, mutation of all three *RB1* family members leads to loss of contact inhibition and outgrowth of fibroblasts into spheres where cell-cell contacts predominate. We present evidence that such outgrowth triggers reprogramming to generate cells with properties of cancer stem cells. Fibroblasts with only a single *RB1* mutation remain contact inhibited; however, if this contact inhibition is bypassed by forcing the $RB1^{-/-}$ cells to form spheres in suspension, cells with properties of cancer stem cells are also generated. These cells not only form tumors in nude mice but also generate differentiated cells. We propose that contact inhibition imposed by the RB1 pathway performs an unexpected tumor suppressor function by preventing cell outgrowth into structures where cells with properties of cancer stem cells can be generated from differentiated somatic cells in advancing cancers.

INTRODUCTION

Solid tumors as well as cancers of hematopoietic origin have been shown to contain a small population of cancer-initiating cells, designated cancer stem cells, that in xenographic transplants are capable of regenerating the heterogeneous population of cancer cells in a tumor (Dalerba et al., 2007; Dick, 2005; Lobo et al., 2007; O'Brien et al., 2007; Trosko, 2006; Zhang and Rosen, 2006). As their name implies, cancer stem cells have some properties of embryonic stem cells (ESCs), including expression of ESC genes and the ability to divide asymmetrically to generate cancer cells while maintaining their number in the tumor. Because such properties are thought to be reserved for stem cells, it has been postulated that cancer stem cells and thus cancers arise from transformation of resident stem cells in tissues. However, in at least some cancers, such as melanoma, cells with cancer stem cell properties appear in advanced tumors, where they have been shown to be important in tumor maintenance/progression (Schatton et

*Correspondence: dcdean01@louisville.edu.

al., 2008; Jordan, 2009). Such cells were less evident in precancerous nevi or early tumors, raising questions regarding the origin of these cells and suggesting that they may be critical for progression of advanced cancer as opposed to cancer initiation.

There is therapeutic interest in cancer stem cells because they have properties distinct from the remainder of the tumor. They express multidrug-resistant transporters, such as Abcg2, that can efflux chemotherapy drugs, and the cells are frequently slow growing or quiescent, affording them relative resistance to therapies that target rapidly growing cancer cells (Zhang and Rosen, 2006; Lobo et al., 2007; Dalerba et al., 2007; Robey et al., 2007; Dirks, 2008). It is suggested that quiescent cancer stem cells that survive cancer treatment may remain dormant for long periods, only to reinitiate proliferation at some point in the future and restore the original tumor (Zhang and Rosen, 2006). Much of the research effort on cancer stem cells has focused on cell surface markers such as CD133 on brain tumors and a CD44-high/CD24-low pattern on breast cancers (Dalerba et al., 2007; Dick, 2005; Lobo et al., 2007; O'Brien et al., 2007; Zhang and Rosen, 2006; Mani et al., 2008; Dirks, 2008). Although such markers have been used to identify and isolate cells with properties of cancer stem cells, substantial differences have been reported in markers not only in cells from different tumors but also among patients with similar tumors (reviewed in Jordan, 2009). Such diversity of markers in cells from patients with similar tumors raises questions as to whether cancer stem cells are derived from a common stem cell progenitor.

A recent study from the Weinberg laboratory has provided evidence that cells with at least some of the properties of stem cells and cancer stem cells can be induced from differentiated somatic cells by overexpression of E box binding transcription factors including Snai, Twist, and Zeb family members (Mani et al., 2008). These transcription factors all have been shown to be overexpressed in carcinomas, where they drive epithelial-to-mesenchymal transition (EMT), which is thought to facilitate a metastatic phenotype in late-stage cancers. However, these new studies demonstrated that overexpression of the EMT transcription factors has a hitherto unanticipated role in initiating a CD44-high/CD24-low pattern on breast epithelial cells, which coincides with their acquisition of properties of stem cells and cancer stem cells. Chang's laboratory has also recently demonstrated that an ESC gene expression module and properties of cancer stem cells can be induced in primary culture keratinocytes, and c-Myc is central to this process (Wong et al., 2008). *c-Myc* amplification is linked to initiation of EMT in breast cancer (Trimboli et al., 2008). Also, c-Myc is a classic target of Wnt, whose signaling triggers EMT at least in part through activation of EMT transcription factors (Neth et al., 2007; Stemmer et al., 2008). Taken together, these studies provide evidence that cells with properties of cancer stem cells can be generated from differentiated somatic cells.

Recent studies have begun to provide evidence that at least some cancers originate in differentiated somatic cells as opposed to stem cells or progenitor cells. One such cancer, retinoblastoma, is a pediatric tumor of the retina and perhaps the best-defined tumor with regard to mutations leading to cancer (MacPherson and Dyer, 2007). Initiation of retinoblastoma in humans appears to require only mutation of both copies of the retinoblastoma tumor suppressor *RB1*. Using a mouse model of retinoblastoma, it has been demonstrated that differentiated horizontal interneurons in the inner nuclear layer of the retina are the target of transformation, as opposed to a stem cell or progenitor cell as previously presumed (Ajioka et al., 2007; te Riele, 2007). While initiation of retinoblastoma appears to involve outgrowth of these differentiated neurons, it is of note that highly aggressive cancer cells (lacking neuronal markers), as well as cells with properties of cancer stem cells, subsequently appear in retinoblastomas (Seigel et al., 2005, 2007; MacPherson and Dyer, 2007). These results in this mouse model of retinoblastoma, taken together with the findings discussed above, raise the possibility that cancer stem cells can be derived from differentiated somatic cells, and that such cells may be somehow generated in advancing tumors.

Beyond retinoblastoma, mutation or inactivation of the RB1 pathway via hyperphosphorylation catalyzed by cyclin-dependent kinases (cdks) occurs in virtually all cancers, suggesting that inhibition of this pathway plays a general role in cancer initiation. A hallmark of all solid tumors is the outgrowth of cancer cells into three-dimensional (3D) structures. The RB1 pathway is crucial for imposing the cell-cycle arrest that mediates cell-cell contact inhibition (Zhang et al., 1999; Sage et al., 2000; Dannenberg et al., 2000), and accordingly fibroblasts in which all three RB1 family members, *RB1*, *RBL1*, and *RBL2*, have been mutated (triple knockouts [TKOs]) lack contact inhibition and grow into 3D colonies or mounds in cell culture (Dannenberg et al., 2000; Sage et al., 2000). We hypothesized that the outgrowth of cells into such spherical structures where cell-cell contacts predominate may play an active role in reprogramming somatic cells to a cancer-stem-cell-like phenotype.

Here, we provide evidence that outgrowth of TKO MEFs into spheres indeed leads to stable reprogramming of the cells to a cancer stem cell phenotype. While fibroblasts containing only an *RB1* mutation retain cell contact inhibition, bypassing this inhibition by forcing the cells to form spheres in suspension leads to similar reprogramming of the $RB1^{-/-}$ cells to a cancer stem cell phenotype. These cells not only divide asymmetrically to produce cancer cells but also generate differentiated cells. Our results provide evidence of a potential pathway for generation of cancer stem cells from differentiated somatic cells as a consequence of tumor outgrowth. Based on these findings, we suggest a novel tumor suppressor function for the RB1 pathway in imposing contact inhibition to prevent outgrowth of differentiated somatic cells into structures where reprogramming to cancer stem cells can occur.

RESULTS

RB1 Family Mutation Allows Outgrowth of Cells into Spheres, Leading to Survival in Suspension and Stable Changes in Cell Morphology

Consistent with their lack of cell-cell contact inhibition, once mouse embryo fibroblasts (MEFs) in which all three *RB1* family members had been mutated (TKOs) became confluent in culture, they began to form 3D colonies or mounds of cells on the plate (Dannenberg et al., 2000; Sage et al., 2000; Figures 1A and 1B). Similar results were seen with cells at passages 4, 11, and 40 and cells from four different litters (results not shown). Subsequently, outgrowth of cells in these mounds led to detachment of the mounds from the culture plate and formation of spheres in suspension (Figures 1C and 1D). This sphere formation was efficient, and with time, most TKO cells on the plate formed spheres. By contrast to TKOs, wild-type MEFs, $RB1^{-/-}$ MEFs, or MEFs with two RB1 family members mutated, $RB1^{-/-}/RBL2^{-/-}$ MEFs, remained contact inhibited, and thus did not form such mounds or spheres (results not shown). The TKO spheres visually resembled embryoid bodies seen when embryonic stem cells are placed in suspension culture (Figures 1C and 1D; Desbaillets et al., 2000), and when transferred to plates that do not permit adherence, these spheres could be maintained for months in suspension. During this period, they increased in size and formed a central cavity (Figure 1E). When the spheres were transferred back to a tissue culture plate that allows adherence of cells, they adhered to the plate, and all of the cells within the spheres migrated back onto the plate, reforming a monolayer (Figures 1F and 1G). Surprisingly, none of the cells in these monolayers resembled TKOs prior to sphere formation—they were smaller and morphologically heterogeneous (compare Figure 1A to Figures 1H and 1I). These sphere-derived TKOs retained this smaller size and distinct morphology as they were passaged in culture, demonstrating a stable morphological transition. We never observed generation of cells with such morphology in TKOs maintained in subconfluent monolayer cultures, even after 40 passages (results not shown).

If a monolayer of TKOs was trypsinized and the resulting cells were placed in suspension culture, spheres did not form, and the single cells began to die after 24 hr in suspension (results

not shown). However, if TKOs from confluent monolayers were scraped from plates (without trypsinization), the cells formed spheres in suspension. Such spheres were indistinguishable in all experiments described below from mound-derived cells that spontaneously detached from confluent TKO cultures. Consistent with their lack of survival in suspension culture, trypsinized TKO did not form colonies in soft agar, nor did they form tumors in nude mice (results not shown).

The above studies suggest that cell-cell contact affords TKO MEFs resistance to death in suspension, and the stable morphological changes imply that the cells are undergoing reprogramming (e.g., differentiation or dedifferentiation) in the context of the spheres.

Sphere Formation in *RB1*$^{-/-}$ MEFs Also Leads to Survival in Suspension and Stable Morphological Changes

As noted above, persistence of contact inhibition in *RB1*$^{-/-}$ MEFs mediated by the other two RB1 family members, RBL1 and RBL2, prevented formation of mounds and in turn spheres in monolayer culture. However, scraping confluent monolayers of TKO cells and placing the cells in suspension culture led to formation of spheres with properties indistinguishable from those seen in spheres derived from mounds that spontaneously detached from confluent plates. Therefore, we postulated that bypassing contact inhibition by scraping confluent *RB1*$^{-/-}$ MEFs from plates and placing them in suspension culture may lead to sphere formation and generation of cells with distinct morphology. Indeed, when scraped from plates, *RB1*$^{-/-}$ MEFs formed spheres in suspension as efficiently as TKOs, and the spheres were indistinguishable morphologically from those formed with TKOs, increased in size, and remained viable for months in culture (results not shown). As with TKO spheres, *RB1*$^{-/-}$ MEF spheres reattached when transferred to a tissue culture plate allowing adhesion, and all cells in the spheres migrated back onto the plate to reform a monolayer; also, as with TKO-sphere-derived cells, *RB1*$^{-/-}$ cells in these monolayers were small, morphologically diverse, and distinct from the original *RB1*$^{-/-}$ MEFs (results not shown). Real-time PCR demonstrated that mRNAs for the other two RB1 family members, RBL1 and RBL2, were initially downregulated in the *RB1*$^{-/-}$ spheres at day 4 in suspension culture, potentially accounting for the loss of contact inhibition in the spheres (Figure 2A). However, RBL2 mRNA expression resumed after day 8 in suspension (Figure 2A), and it was maintained in sphere-derived cells migrating back onto a culture dish (see Figure S1 available online). Taken together, the above results suggest that bypassing cell-cell contact inhibition in monolayer culture and forcing *RB1*$^{-/-}$ MEFs to form spheres also leads to stable changes in cell morphology. It is of note that we observed similar sphere formation with wild-type MEFs, and RB1 family mRNA expression was not downregulated during sphere formation (Figure S2), suggesting that sphere formation per se does not require downregulation of the RB1 family.

Sphere Formation in TKOs and *RB1*$^{-/-}$ MEFs Leads to Expression of ESC Genes

Because cells in the spheres undergo a stable change in morphology that may reflect reprogramming, we used real-time PCR to examine expression of ESC gene mRNAs in cells derived from spheres after 2 weeks in suspension culture, and these results were compared to cells maintained as subconfluent monolayers. These mRNAs included Oct-4, Nanog, Sox2, and Klf4, whose expression is associated with reprogramming of fibroblasts to a stem cell phenotype (Figure 2A). Expression of both Oct-4 and Nanog mRNA increased during a time course of *RB1*$^{-/-}$ MEF sphere formation in suspension culture (Figure 2B). To confirm Oct-4 protein expression, spheres were immunostained for Oct-4. After 4 days in suspension, we only observed low-level cytoplasmic staining for Oct-4 (Figure 2C). Even though this cytoplasmic staining was dependent upon the primary antibody, little or no Oct-4 mRNA was detected at this time (Figure 2B). Thus, this cytoplasmic immunostaining does not appear to be specific for Oct-4, and as suggested previously, it may arise from expression of Oct-4 pseudogenes

(Lengner et al., 2007). After 8 days in suspension culture, nuclear immunostaining for Oct-4 became evident in clusters of cells in the spheres; this nuclear immunostaining further increased at 24 days, and during this period there was also an increase in the level of Oct-4 mRNA by real-time PCR (Figures 2B and 2C). Nanog is a downstream target of Oct-4, and thus its expression is a functional readout of Oct-4 activity. The level of Nanog mRNA paralleled that of Oct4 during this time course of sphere culture (Figure 2B). In addition to these ESC-specific genes, we also noted upregulation of other genes associated with stem cells in both TKO and *RB1*$^{-/-}$ MEF spheres (Figure 2D and Figure S1). A similar pattern of expression of ESC-associated genes was maintained as sphere-derived *RB1*$^{-/-}$ cells migrated out of spheres to reform a monolayer on tissue culture dishes (Figure S3). These results suggested that at least some cells in the spheres are re-expressing ESC-associated genes. Because re-expression of such genes in fibroblasts is sufficient to reprogram the cells to pluripotency, it was possible that the re-expression of these genes that we observed in the spheres was inducing reprogramming of the fibroblasts that was reflected in the stable changes in morphology. It is also of note that mRNAs for CD44 and CD133 were induced, and CD24 mRNA was downregulated (Figure 2D). This is a pattern of expression seen in some cancer stem cells, raising the question as to whether some of the cells in the spheres may have cancer stem cell properties.

A Subset of Cells with Properties of a Side Population Is Generated in TKO and *RB1*$^{-/-}$ MEF Spheres

Multipotential stem cells in bone marrow and other tissues have been characterized as a side population (SP) based on their properties compared to the major population (MP) of cells present (reviewed in Challen and Little, 2006). Also, these SP characteristics are shared by a small subset of cells in tumors, referred to as cancer stem cells, that can recapitulate the tumor heterogeneity in transplantation assays (Hirschmann-Jax et al., 2005). In addition to tumor cells, cancer stem cells can also give rise to differentiated cells (Dirks, 2008). Because of the re-expression of ESC genes and the stable changes in morphology seen in sphere-derived cells, we wondered if sphere formation might be reprogramming the RB1 pathway mutant fibroblasts to generate SP cells with properties of stem cells or cancer stem cells. Among the characteristics of SP cells is expression of multi-drug-resistant transporters such as Abcg2 and the accompanying ability to exclude Hoechst 33342 dye (and chemotherapy drugs) (Robey et al., 2007).

We began by examining wild-type MEFs, TKOs maintained as subconfluent monolayers, and TKOs derived from spheres for Hoechst dye exclusion and cell surface expression of Abcg2 and CD133. We found that MEFs and TKOs maintained as subconfluent monolayers did not exclude Hoechst dye or express Abcg2 or CD133 on their surface (Figures 3A and 3C; results not shown). However, ~10% of sphere-derived TKOs at P0 were Hoechst−, Abcg2+, CD133 + (Figures 3B and 3C). Notably, these Hoechst−, Abcg2+, CD133+ cells were much smaller (~5 μm in diameter) than the MP, which consisted of Hoechst+, Abcg2−, CD133− cells (>10 μm). We then examined *RB1*$^{-/-}$ cells for SP properties. As with wild-type MEFs, the *RB1*$^{-/-}$ MEFs in monolayer culture did not display SP properties (Figure 3C); however, cells derived from *RB1*$^{-/-}$ MEF spheres showed a similar SP population to TKOs (Figure 3C).

Another property of SP cells is asymmetric division to give rise to MP cells, while maintaining their own number (Dalerba et al., 2007; Dick, 2005; Lobo et al., 2007; O'Brien et al., 2007; Trosko, 2006; Zhang and Rosen, 2006; Knoblich, 2008). We sorted sphere-derived monolayers of TKOs (Figure S4), leading to a uniform population of small Hoechst−, Abcg2+, CD133+ cells, denoted SP. While noHoechst+,Abcg2−,CD133−cells (denoted MP) were evident in the sorted SP cells initially, MP cells appeared after 2 days in culture, and by this time they comprised the majority of the culture (Figure 3D). The percentage of MP cells increased further

by day 8 in culture (Figure 3D). We then followed SP cells derived from *RB1*$^{-/-}$ MEFs in culture. As with TKOs, these cells also gave rise to MP cells while maintaining their original number (Figure 3D). Next, we analyzed single SP cells from *RB1*$^{-/-}$ MEFs in culture. As with the entire sorted population, during the course of 5 days, the single SP cells gave rise toMPcells, but their original number remained constant (Figures 3E–3H and 3M).

Next, we analyzed the sorted MP cells. These cells were proliferative, but they did not appear to divide asymmetrically to give rise to SP cells (Figure 3D). Indeed, we followed five isolated MP cells, and we only observed symmetrical division to yield MP cells (Figures 3I–3M). Taken together, it appears that SP cells from both TKO and *RB1*$^{-/-}$ spheres give rise to MP cells via asymmetric division, and that the MP cells in turn divide symmetrically to increase their number in the population.

It Is the Hoechst−, Abcg2+, CD133+ SP Cells that Express ESC Markers

The stem cell characteristics attributed to SP populations in tissues, together with the stem cell property of asymmetric division shown above with the sphere-derived SP cells, led us to ask if the SP cells correspond to the population of cells in the sphere that re-express ESC genes. Gene expression in sorted SP and MP populations of cells derived from spheres was compared to embryonic stem cells using real-time PCR. The SP cells from spheres expressed mRNAs for stem cell markers in levels similar to those seen in ESCs (Figure 4A). These markers included Oct-4, Sox2, c-*myc*, and Klf-4, whose retroviral re-expression is sufficient for reprogramming of MEFs to pluripotency (Takahashi and Yamanaka, 2006; Okita et al., 2007; Wernig et al., 2007; Jaenisch and Young, 2008). Conversely, there was little expression of the stem cell mRNAs in the MP cells. These results suggest that the Oct-4+ and Nanog+ cells we observe in spheres correspond to SP cells, and that as SP cells divide asymmetrically ESC genes are silenced in the MP daughter cells.

Zeb1 mRNA Is Induced in SP Cells, and This Is Associated with Downregulation of E-cadherin mRNA, Induction of Smooth Muscle Actin mRNA, and a CD44-High/CD24-Low mRNA Expression Pattern

Overexpression of E box binding transcriptional repressors including Snai, twist, and Zeb family members classically leads to repression of E-cadherin (Cdh1) and EMT, and Snai1 repression of E-cadherin and EMT appears to be mediated at least in part through induction of Zeb1 and Zeb2 (Peinado et al., 2007). Recent studies have demonstrated that overexpression of these EMT factors can also trigger a CD44-high/CD24-low pattern on epithelial cells, which is associated with the somatic cells acquiring stem cell and cancer stem cell properties (Mani et al., 2008). Therefore, we wondered whether expression of these EMT transcription factors was induced in the sphere-derived SP cells. Using real-time PCR, we found that Zeb1 (but not Zeb2, Snai1, or Snai2) mRNA was induced in SP cells compared to MP cells (Figure 4B), and that Zeb1 mRNA increased in a time course of sphere formation in *RB1*$^{-/-}$ MEFs similar to that seen with Oct-4 and Nanog mRNA (Figure 2B and Figure 4C). Consistent with upregulation of Zeb1, smooth muscle actin mRNA was induced in SP cells, whereas E-cadherin mRNA was diminished (Figure 2B), indicating that SP cells are mesenchymal in gene expression compared to MP cells.

Next, we asked whether overexpression of Zeb1 mRNA might coincide with induction of CD44 mRNA and downregulation of CD24 mRNA in SP cells. Indeed, we found that CD44 mRNA was induced in SP cells, whereas CD24 mRNA was diminished (Figure 4B). Flow cytometry demonstrated a similar CD44/CD24 pattern on the cell surface (results not shown). In addition to this CD44-high/CD24-low mRNA pattern in the SP cells, it is of note that CD133 mRNA and protein were also induced in the SP cells, along with Zeb1 mRNA (Figure 4A).

Both Zeb1 and Zeb2 are expressed in wild-type MEFs (Liu et al., 2007, 2008), and we were unable to detect CD44 mRNA in these cells, but CD24 mRNA was expressed (Figure 4D). We then used lentiviral shRNA constructs to knock down Zeb1 and Zeb2 in these cells (Figure S5) to determine whether either of these EMT transcription factors might be important in maintaining repression of CD24. We found that knockdown of Zeb2 had little effect on the level of CD24 mRNA; however, CD24 mRNA was significantly induced with Zeb1 knockdown (Figure 4D). These results provide evidence that Zeb1 is necessary to maintain repression of CD24.

Zeb1 Expression Is Required for Viability of SP Cells and Proliferation of MP Cells Derived from *RB1*$^{-/-}$ MEF Spheres

Zeb1 was knocked down using lentivirus shRNA in cells prior to sphere formation and in SP and MP cells derived from spheres (Figures S5–S8). This knockdown of Zeb1 led to induction of the cyclin-dependent kinase inhibitors p15INK4b and p21CDKN1a and growth arrest in monolayer cells prior to sphere formation (Figure S7). However, these cells were still able to form spheres in suspension, and these spheres re-expressed ESC genes such as Oct4 and Nanog, suggesting that Zeb1 is not required for sphere formation or for re-expression of these ESC genes. However, the spheres that formed were small, and they did not increase in size during suspension culture.

Knockdown of Zeb1 in isolated SP cells prevented the cells from giving rise to MP cells, and it led to rounding of the cells within 18 hr after infection; by day 5 following infection the cells were no longer viable (Figure S8). By contrast, MP cells did not round up nor was there a significant loss in viability with Zeb1 knockdown. However, the cells did not proliferate, and they accumulated multiple nuclei. These results demonstrate an important role for Zeb1 in the survival of isolated SP cells and the proliferation of MP cells.

RB1$^{-/-}$ and TKO MEF Spheres Express Markers of All Three Embryonic Layers

The appearance of SP cells expressing ESC markers in TKO and *RB1*$^{-/-}$ MEF spheres, together with the diverse morphology seen in cells derived from these spheres (Figure 1H), led us to ask whether there was evidence of differentiation in the spheres (e.g., analogous to differentiation seen when embryonic stem cells form embryoid bodies). We used real-time PCR to analyze mRNA expression in spheres and in cells that had been allowed to migrate from spheres and reform monolayers on tissue culture plates. Similar induction of mRNAs for markers of all three embryonic layers was seen in spheres and sphere-derived cells (Figure 5A–5C, Figures S1, S3, and S9). These markers included important developmental transcription factors such as GATA4, T, Msx1, Foxa2, MyoD, Ascl2, PDX1, PPARγ, and islet1, and components of development signaling pathways including TGF-β/BMP, notch, wnt, and FGF. However, they also included markers of terminal differentiation such as cardiac actin, myosin heavy chain, osteocalcin, aggrecan, E-cadherin, transferin, α-fetoprotein (AFP), myelin basic protein, GFAP, tyrosine hydroxylase, β-III tubulin, NCAM, Neurog2, Col9a1, CD19, CD3, CD4, and CD8.

Next, spheres were fixed and sectioned for immunostaining. The perimeter of embryoid bodies formed from ESCs contain early endodermal cells characterized by expression of AFP and GATA-4, and this region is a site of hematopoietic and endothelial differentiation resembling embryonic yolk sac blood islands (Burkert et al., 1991). We noted a band of cells around the perimeter of *RB1*$^{-/-}$ MEF spheres that resembled endodermal cells (Figure 6A), and these cells immunostained for AFP (Figures 6D and 6E). This region also immunostained for GATA-4 and mRNAs for GATA-4, and the early endodermal transcription factors Foxa2, PDX1, and Isl1 were also induced in spheres and sphere-derived cells (Figure 5, Figure S1, and S9). The region also contained a number of cells with eosinophilic cytoplasm (Figure 6B), and these

cells immunostained for α-globin, indicating that they are erythroid (Figure 6F–6H and Figure S10). These cells also were brightly stained with benzidine/peroxide, which is specific for hemoglobin (Figure 6C). While most of these globin+ cells were nucleated, some of the cells lacked nuclei (Figure 6H and Figure S10), implying that they may be progressing from erythroblast-like progenitors toward erythrocytes in the spheres. This perimeter region of the spheres also contained cells with elongated morphology resembling endothelial cells (Figures 6A and 6B), and indeed these cells immunostained for the endothelial marker CD31 (Figures 6I and 6J). Although less abundant than the globin+ cells, cells with morphology of other hematopoietic lineages were also evident (Figure S10). Flow cytometry of total sphere-derived cells revealed that approximately 2% of the population expressed the hematopoietic stem cell marker CD34 and approximately 1%expressed the B cell marker CD19 (results not shown). CD34 and CD19 mRNAs were also induced in the spheres (Figure 5C, Figures S1, and S9). Taken together, our results provide evidence that, as in embryoid bodies, the perimeter of the spheres is a site of hematopoietic/endothelial differentiation.

Cells interior to the globin+ cells in spheres displayed epithelial-like morphology (Figure 6C), and these cells expressed the early epithelial marker E-cadherin (Cdh1) (Figure 6K). Cdh1 mRNA was also induced in the spheres and sphere-derived cells, as was mRNA for the epithelial progenitor marker Ker15 (Figures S1 and S9). We also noted immunostaining for the neuronal marker β-III tubulin (Figure 6L). These β-III tubulin+ cells were generally in clusters or spherical structures. Immunostaining for all of the markers of differentiation increased in a time-dependent fashion from 4 days in suspension culture out to at least 24 days. And by 24 days, a higher percentage of the β-III tubulin+ cells exhibited elongated morphology characteristic of neurons.

Similar staining for globin, AFP, and CD31 was also seen in the periphery of spheres derived from TKO cells (results not shown). Again, β-III tubulin+ cells were found primarily in clusters containing cells with neuronal morphology, and cells in these clusters also expressed α-tyrosine hydroxlyase (a marker of dopaminergic neurons) (Figure S11). Cells surrounding some of these neuronal clusters showed elongated projections and the immunostained for both tyrosine hydroxylase and the motor neuron marker Isl1 (Figure S11). In addition to these neuronal markers, immunostaining for markers of oligodendrocytes (myelin basic protein) and glia/astrocytes (GFAP) was also evident in distinct regions of the spheres (Figure S11). Expression of these neural markers is consistent with the induction of mRNA for various neural markers in the spheres and sphere-derived cells (Figure 5B, Figures S1, and S9). Based on these real-time PCR and immunostaining results, we conclude that in addition to generation of cells with SP properties, sphere formation with *RB1*$^{-/-}$ and TKO MEFs is triggering generation of cells expressing markers of all three embryonic layers. Attempts to differentiate SP cells in monolayer culture led only to production of MP cells lacking expression of ESC genes or differentiation markers. In these experiments cells were cultured on laminin, fibronectin, gelatin, or plastic and exposed to various differentiation protocols for ESCs. However, isolated SP cells could be used to reform spheres, which again re-expressed ESC genes along with the series of genes and transcription factors indicative of formation of cells representative of all three embryonic layers (Figure S12). These results provide evidence that SP cells can give rise to differentiated cells in the spheres, and they suggest that the niche within the sphere (which may be lost in monolayer culture) may be important for SP maintenance/differentiation.

SP Cells Form Tumors in Nude Mice

Because mutation of *RB1* or inhibition of the RB1 pathway is a hall-mark of cancer and the SP cells show a pattern of cell surface expression seen on some cancer stem cells (e.g., CD44-high, CD24-low, CD133-high, Abcg2+) we wondered whether the SP cells formed during sphere formation may have the tumor-forming capability of cancer stem cells. To determine

whether tumorigenic cells were being generated by sphere formation, small spheres of TKO or *RB1*$^{-/-}$ MEFs after 2 weeks in suspension culture were injected subcutaneously into the hind limb of nude mice. Tumors arose from these spheres. The tumors were all spindle cell sarcomas, but they also contained scattered spherical whorls with eosinophilic centers (Figure 7C). As a negative control, tumors did not arise following injection of 100,000 TKO MEFs that were trypsinized from subconfluent monolayers and injected into the nude mice (results not shown). To determine if this tumor-forming activity was maintained in sphere-derived cells that had migrated from spheres to reform a monolayer, we trypsinized such monolayers of sphere-derived TKOs or *RB1*$^{-/-}$ MEFs and injected 50,000 cells into the nude mice. Tumors formed with both cell types, and they were histologically indistinguishable from those formed with the spheres (Figure 7C, Figures S13, and S14). In each case, the tumors again were spindle cell sarcomas, and they also contained the sphere-like whorls with eosinophilic centers (Figure 7C and Figure S13). These whorls were devoid of cancer cells, and they appeared histologically similar to regions evident in spheres in culture, which expressed markers of neuronal differentiation (Figure S11). Indeed, immunostaining of tumor sections revealed that these whorls expressed β-III tubulin, and as with spheres in culture, no other regions of the tumor expressed β-III tubulin (Figure S13).

Next, we injected different numbers of sorted SP and MP cells into nude mice to assess which population was tumorigenic. Two independent experiments were performed with two injections of each cell number in the following experiments. Initially, 50,000, 20,000, 5,000, and 1,000 MP cells were injected. While tumors formed with each injection of 50,000 MP cells (523 ± 93 mg after 31 days), no tumors were observed in any injection with 20,000 or fewer MP cells, even after 2 months (Figure 7B). Next, we injected 5,000, 2,000, 500, and 100 SP cells. Tumors formed with every injection of the SP cells, and these tumors grew rapidly (813 ± 279 mg at 3 weeks with 100 SP cells injected; Figure 7A). Based on these results, we concluded that SP cells are the primary initiators of tumor formation among the sphere-derived cells. However, it is of note that the tumors formed from SP and MP cells were histologically distinct (Figures 7D–7H). Although the MP tumors were spindle cell sarcomas, they lacked the β-III tubulin+ spherical whorls seen with injection of unsorted sphere-derived cells. Additionally, the number of whorls seen in the SP cell tumors was greater than that seen with the mixed population of sphere-derived cells (Figures 7E–7H). The SP tumors also contained clusters of cells expressing nuclear Oct-4 and Nanog scattered throughout the tumor (Figures 7I–7L), suggesting that SP cells are maintained in the forming tumor. These results provide evidence that the SP cells not only can give rise to cells expressing markers of differentiation in the spheres and in the nude mice but also are tumorigenic and thus appear to be functioning as cancer stem cells. MP cells in high numbers were able to give rise to cancer cells in the mice, but not the differentiated cells, implying that the MP cells represent cancer cells generated by the SP cells.

DISCUSSION

Beyond retinoblastoma, *RB1* is also frequently mutated in osteosarcoma and small-cell lung cancer, and patients heterozygous for *RB1* have significantly increased risk for developing these cancers (Sábado Alvarez, 2008; Kansara and Thomas, 2007). Indeed, tumors derived from TKO and *RB1*$^{-/-}$ MEFs contained cells resembling spindle cell sarcomas. Moreover, the RB1 family is regulated by phosphorylation mediated by cdks, and in tumors where *RB1* is not mutated the pathway is inactivated by hyperphosphorylation of family members (Kaye, 2002; Du and Pogoriler, 2006; Frolov and Dyson, 2004; Lowe and Sherr, 2003). Thus, loss of the RB1 pathway appears to be a hallmark of most if not all cancers. The loss of cell-cycle control when the RB1 pathway is disrupted is thought to play an important role in the initiation of tumor cell proliferation. However, beyond tumor expansion, we propose that the loss of cell contact inhibition when the RB1 pathway is inhibited leads to outgrowth into sphere-like

structures where cell-cell contacts predominate, and these conditions in the advancing cancer trigger reprogramming of somatic cells to cells with properties of cancer stem cells (Figure 7M). Even though *RB1*$^{-/-}$ MEFs were contact inhibited in monolayer culture, they could still form spheres when placed in suspension culture and generate SP cells with properties of cancer stem cells. While similar spheres formed with wild-type MEFs and differentiated cells were generated in these spheres (results not shown), neither these wild-type spheres nor cells derived from the spheres were able to form tumors in nude mice, emphasizing the importance of *RB1*$^{-/-}$ mutation in generation of tumor cells in the spheres. Our studies are consistent with previously published results implying that cells with properties of cancer stem cells can be generated from somatic cells, and they suggest a pathway linked to tumor outgrowth for generation of such cells in more advanced tumors.

Interestingly, the SP cells with properties of cancer stem cells isolated from spheres of MEFs mutant in the RB1 pathway expressed ESC genes including Oct-4, Sox-2, Nanog, Klf4, and c-*myc*, and this was accompanied by induction of genes in pathways known to be important for ESCs maintenance such as TFG-β/BMP, Wnt, Notch, hedgehog, and FGF. To our knowledge, this is the first example that silenced endogenous ESC genes such as Oct-4 and Nanog can be reactivated in differentiated somatic cells. Beyond production of cancer cells, a number of cells in TKO and *RB1*$^{-/-}$ MEF spheres express markers representative of all three embryonic layers, reminiscent of what occurs in embryoid bodies derived from ESCs. It has been demonstrated previously that cancer stem cells can also give rise to differentiated cells along with cancer cells (Dirks, 2008). While we are unsure of the steps involved in the differentiation process in the spheres, it is interesting to speculate that sphere formation is reprogramming differentiated somatic cells with a mutant RB1 pathway back to a multipotential phenotype capable of generating differentiated cells, and that these progenitor cells correspond to the SP. In support of this notion, isolated SP cells could reform spheres and again induce ESC genes and a series of differentiation markers. Furthermore, injection of SP cells into nude mice led not only to production of what appeared to be a homologous population of cancer cells (spindle cell sarcoma), but also to neuronal cells segregated in whorls in a niche distinct from the cancer cells. While wild-type ESCs form teratomas when injected into nude mice, it is of note that TKO ESCs formed spherical structures expressing early neuronal markers in nude mice (Dannenberg et al., 2000). In this way, the SP cells derived from TKO and *RB1*$^{-/-}$ MEF spheres appear to resemble TKO ESCs.

Recent studies have demonstrated that overexpression of EMT transcription factors in epithelial cells can trigger the CD44-high/CD24-low expression pattern that is thought to be important for generation of breast cancer stem cells (Mani et al., 2008). We also observed induction of CD44 and diminished expression of CD24 mRNAs in SP cells. While we did not see a change in expression of the EMT factors Snai1, Snai2, or Zeb2, Zeb1 mRNA expression was induced in SP versus MP cells. Additionally, this elevated expression of Zeb1 was accompanied by repression of E-cadherin and induction of smooth muscle actin in the SP cells, suggesting a relatively mesenchymal expression pattern compared to MP cells. Zeb1 is directly repressed by E2F-RB1 family complexes, which appears to limit its expression to proliferating cells in vivo (Liu et al., 2007, 2008), and the downregulation of RBL1 and RBL2 initially during sphere formation may facilitate this induction during sphere formation.

Inspection of the CD24 promoter region revealed multiple consensus Zeb1 binding sites, suggesting that CD24 may be a direct target of Zeb1 repression in SP cells. Indeed, knockdown of Zeb1 but not Zeb2 led to induction of CD24 mRNA, suggesting that Zeb1 is important in repressing CD24 expression. Zeb1 expression is tightly linked to cell proliferation in vivo, and it directly represses the cdk inhibitors p15INK4b and p21CDKN1a, which inhibit the cell cycle (Liu et al., 2008 and references therein). Heterozygous mutation of *Zeb1* is sufficient for induction of both of these genes, and it leads to premature senescence of MEFs in culture, and

induction of p15INK4b in *Zeb1*$^{-/-}$ cells in vivo is linked to diminished mesenchymal and CNS progenitor cell proliferation during development with accompanying developmental defects (Liu et al., 2008). Knockdown of Zeb1 inhibited growth of spheres in suspension, it prevented generation of MP cells from isolated SP cells, and it led to the eventual loss of SP cell viability in culture. In this regard, it is of note that the *Drosophila* homolog of Zeb1, Zfh1, was recently shown to be necessary for viability of stem cells in the testis (Leatherman and Dinardo, 2008), implying an important role in normal stem cell viability.

EXPERIMENTAL PROCEDURES

Cells and Cell Culture

RB1 family mutant mouse embryo fibroblasts and control wild-type MEFs were kind gifts from T. Jacks, J. Sage, and G. Leone. TKOs derived from four separate embryos were used in the experiments described here with similar results. Cells were analyzed beginning at passage 4, but similar results were also seen at passage 11. The cells were cultured in DMEM with 10% heat-inactivated fetal bovine serum. Mouse embryonic stem cells were obtained from M. Ratajczak. One unit/ml of LIF (Chemicon) was added to embryonic stem cell cultures.

Immunohistochemistry

Slides were immunostained as described previously (Liu et al., 2008). All primary and secondary antibodies are described in Tables S1–S3. Primary antibodies were incubated at 4° C overnight, and after three washes with PBS, slides were incubated at 1:200–500 dilution with secondary antibodies conjugated with either Cy3 or Alexa Fluor 488 at room temperature for 60 min. After three washes with PBS, slides were mounted with coverslips using either anti-fade medium Permount (Fisher) or Vectashield DAPI medium (Vector Laboratories, Inc.), and images were captured either with an Olympus confocal microscope or with a Zeiss fluorescent microscope.

Tumor Formation in Nude Mice

Either small spheres ~1 mm in diameter, after 2 weeks in suspension culture, or trypsinized monolayers of cells derived from spheres were injected subcutaneously into the hind limb of Balb/c nude mice as described (Telang et al., 2006). Tumors were fixed in 10% buffered formalin, embedded in paraffin, sectioned at 5 μm, and stained with H&E or used for immunostaining (Liu et al., 2008).

Identification and Isolation of SP and MP Cells

Cells were trypsinized from tissue culture plates, suspended in prewarmed DMEM containing 2% FBS and 10 mM HEPES, and stained with 5 μg/ml of Hoechst 33342 dye (Molecular Probes) for 90 min at 37°C. Cells were then washed and resuspended in HBSS containing 2% FBS and 10 mM HEPES. Before cell sorting, 2 μg/ml propidium iodide (Sigma) was added to exclude nonviable cells. SP cells were identified and isolated by MoFlo cell sorter (Dako; Carpinteria, CA) after excitation of the Hoechst dye with a 350 nm UV laser (100 mW power was used). Fluorescence light emitted by cells was directed toward a 510 nm DCLP dichroic mirror and collected simultaneously by two independent detectors following a 450/65 nm and a 670/30 nm band pass filters, respectively. Cells were analyzed on a linearly amplified fluorescence scale.

For immunostaining, Hoechst 33342-treated cells were spun down, washed twice with PBS, and incubated either with rat anti-Abcg2 (1:20) or mouse anti- CD133 (1:50) for 1 hr at room temperature. No blocking serum was used. Cy3-conjugated anti-rat IgG (1:200) (Chemicon) and Alexa Fluor 488-conjugated anti-mouse IgG (1:200) (Molecular Probes) were the

secondary antibodies for anti-Abcg2 and anti-CD133, respectively. Images were captured with an Olympus confocal microscope.

RNA Extraction and Real-Time PCR

RNA was extracted using TRIzol, and cDNA was synthesized using the Invitrogen RT kit (Invitrogen), and SYBR Green real-time PCR was performed using a Stratagene Mx3000P Real-Time PCR system (Liu et al., 2008). PCR primers are described in Table S1. A mouse stem cell real-time PCR Array was also analyzed (SuperArray, APMM-405). Three independent samples, each in triplicate, were analyzed for each real-time PCR condition.

Supplementary Material

Refer to Web version on PubMed Central for supplementary material.

ACKNOWLEDGMENTS

We thank T. Jacks, J. Sage, and G. Leone for TKOs, *RB1* null, *RB1/RBL2* double null, and littermate control wild-type MEFs; D. Darling for antibodies; J. Sundberg for comments on tumor pathology; and Qiutang Li for assistance with Zeb1 and Zeb2 lentivirus shRNA constructs. These studies were supported in part by grants from the NIH.

REFERENCES

Ajioka I, Martins RAP, Bayazitov IT, Donovan S, Johnson DA, Frase S, Cicero SA, Boyd K, Zakharenko SS, Dyer MA. Differentiated horizontal interneurons clonally expand to form metastatic retinoblastoma in mice. Cell 2007;131:378–390. [PubMed: 17956737]

Burkert U, Ruden T, Wagner EF. Early fetal hematopoietic development from in vitro differentiated embryonic stem cells. New Biol 1991;3:698–708. [PubMed: 1721533]

Challen GA, Little MH. A side order of stem cells: the SP phenotype. Stem Cells 2006;24:3–12. [PubMed: 16449630]

Dalerba P, Cho RW, Clarke MF. Cancer stem cells: models and concepts. Annu. Rev. Med 2007;58:267–284. [PubMed: 17002552]

Dannenberg J-H, van Rossum A, Schuijff L, te Riele H. Ablation of the retinoblastoma gene family deregulates G1 control causing immortalization and increased cell turnover under growth-restricting conditions. Genes Dev 2000;14:3051–3064. [PubMed: 11114893]

Desbaillets I, Ziegler U, Groscurth P, Gassmann M. Embryoid bodies: an in vitro model of mouse embryogenesis. Exp. Physiol 2000;85:645–651. [PubMed: 11187960]

Dick JE. Acute myeloid leukemia stem cells. Ann. N Y Acad. Sci 2005;1044:1–5. [PubMed: 15958691]

Dirks PB. Brain tumor stem cells: bringing order to the chaos of brain cancer. J. Clin. Oncol 2008;26:2916–2923. [PubMed: 18539973]

Du W, Pogoriler J. Retinoblastoma family genes. Oncogene 2006;25:5190–5200. [PubMed: 16936737]

Frolov MV, Dyson NJ. Molecular mechanisms of E2F-dependent activation and pRB-mediated repression. J. Cell Sci 2004;117:2173–2181. [PubMed: 15126619]

Hirschmann-Jax C, Foster AE, Wulf GG, Goodell MA, Brenner MK. A distinct “side population” of cells in human tumor cells: implications for tumor biology and therapy. Cell Cycle 2005;4:203–205. [PubMed: 15655356]

Jaenisch R, Young R. Stem cells, the molecular circuitry of pluripotency and nuclear reprogramming. Cell 2008;132:567–582. [PubMed: 18295576]

Jordan C. Cancer stem cells: controversial or just misunderstood? Cell Stem Cell 2009;4:203–205. [PubMed: 19265659]

Kansara M, Thomas DM. Molecular pathogenesis of osteosarcoma. DNA Cell Biol 2007;26:1–18. [PubMed: 17263592]

Kaye FJ. RB and cyclin dependent kinase pathways: defining a distinction between RB and p16 loss in lung cancer. Oncogene 2002;21:6908–6914. [PubMed: 12362273]

Knoblich JA. Mechanisms of asymmetric stem cell division. Cell 2008;132:583–597. [PubMed: 18295577]

Leatherman JL, Dinardo S. Zfh-1 controls somatic stem cell self-renewal in the *Drosophila* testis and nonautonomously influences germline stem cell self-renewal. Cell Stem Cell 2008;3:44–54. [PubMed: 18593558]

Lengner CJ, Camargo FD, Hochedlinger K, Welstead GG, Zaidi S, Gokhale S, Scholer HR, Tomilin A, Jaenisch R. Oct4 expression is not required for mouse somatic stem cell self-renewal. Cell Stem Cell 2007;1:403–415. [PubMed: 18159219]

Liu Y, Costello M, Hagashi T, Darling DS, Dean DC. The zinc Finger transcription factor, ZFHX1A, is linked to cell proliferation by the Rb family/E2F pathway. Biochem. J 2007;408:79–85. [PubMed: 17655524]

Liu Y, El-Nagger S, Darling DS, Higashi Y, Dean DC. Zeb1 links epithelial-mesenchymal transition and cellular senescence. Development 2008;235:579–588. [PubMed: 18192284]

Lobo NA, Shimono Y, Clarke MF. The biology of cancer stem cells. Annu. Rev. Cell Dev. Biol 2007;23:675–699. [PubMed: 17645413]

Lowe SW, Sherr CJ. Tumor suppression by INK4a-Arf, progress and puzzles. Curr. Opin. Genet. Dev 2003;13:77–83. [PubMed: 12573439]

MacPherson D, Dyer MA. Retinoblastoma: from the two-hit hypothesis to targeted chemotherapy. Cancer Res 2007;67:7547–7550. [PubMed: 17699756]

Mani SA, Guo W, Liao MJ, Eaton EN, Ayyanan A, Zhou AY, Brooks M, Reinhardt F, Zhang CC, Shipitsin M, et al. The epithelial-mesenchymal transition generates cells with properties of stem cells. Cell 2008;133:704–715. [PubMed: 18485877]

Neth P, Ries C, Karow M, Egea V, Ilmer M, Jochum M. The Wnt signal transduction pathway in stem cells and cancer cells: influence on cellular invasion. Stem Cell Rev 2007;3:18–29. [PubMed: 17873378]

O'Brien CA, Pollett A, Gallinger S, Dick JE. A human colon cancer cell capable of initiating tumor growth in immunodeficient mice. Nature 2007;225:106–110.

Okita K, Ichisaka T, Yamanaka S. Generation of germlinecompetent induced pluoripotent stem cells. Nature 2007;448:260–262. [PubMed: 17637646]

Peinado H, Olmeda D, Cano A. Snail, Zeb and bHLH factors in tumor progression: an alliance against the epithelial phenotype? Nat. Rev. Cancer 2007;7:415–428. [PubMed: 17508028]

Robey RW, Polgar O, Deeken J, To KW, Bates SE. ABCG2: determining its relevance to clinical drug resistance. Cancer Metastasis Rev 2007;26:39–57. [PubMed: 17323127]

Sábado Alvarez C. Molecular biology of retinoblastoma. Clin. Transl. Oncol 2008;10:389–394. [PubMed: 18628066]

Sage J, Mulligan GJ, Attardi LD, Miller A, Chen S, Williams B, Theodorou E, Jacks T. Targeted disruption of the three Rb-related genes leads to loss of G(1) control and immortilization. Genes Dev 2000;14:3037–3050. [PubMed: 11114892]

Schatton T, Murphy GF, Frank NY, Yamaura K, Waaga-Gassser AM, Gassar M, Zhan Q, Jordan S, Duncan LM, Wesiharpt C, et al. Identification of cells initiating human melanomas. Nature 2008;451:345–349. [PubMed: 18202660]

Seigel GM, Campbell LM, Narayan M, Gonzalez-Fernandez F. Cancer stem cell characteristics in retinoblastoma. Mol. Vis 2005;11:729–737. [PubMed: 16179903]

Seigel GM, Hackam AS, Ganguly A, Mandell LM, Gonzalez-Fernandez F. Human embryonic and neuronal stem cell markers in retinoblastoma. Mol. Vis 2007;13:823–832. [PubMed: 17615543]

Stemmer V, de Craene B, Berx G, Belrens J. Snail promotes Wnt target gene expression and interacts with beta-catenin. Oncogene 2008;27:5075–5080. [PubMed: 18469861]

Takahashi K, Yamanaka S. Induction of pluripotent stem cells from mouse embryonic and adult fibroblasts cultures by defined factors. Cell 2006;126:663–676. [PubMed: 16904174]

Telang S, Yalcin A, Clem AL, Bucala R, Lane AN, Eaton JW, Chesney J. Ras transformation requires metabolic control by 6-phosphofructo-2-kinase. Oncogene 2006;25:7225–7234. [PubMed: 16715124]

te Riele H. Retinoblastoma teaches a new lesson. Cell 2007;131:227–229. [PubMed: 17956722]

Trimboli AJ, Fukino K, de Bruin A, Wei G, Tanner SM, Creasap N, Rosol TJ, Robinson ML, Eng C, Ostrowski MC, Leone G. Direct evidence for epithelial-mesenchymal transitions in breast cancer. Cancer Res 2008;68:937–945. [PubMed: 18245497]

Trosko JE. From adult stem cells to cancer stem cells: Oct-4 gene, cell-cell communication, and hormones during tumor promotion. Ann. N Y Acad. Sci 2006;1089:36–58. [PubMed: 17261754]

Wernig M, Meissner A, Foreman R, Brambrink T, Ku M, Hochedlinger K, Bernstein BE, Jaenisch R. In vitro reprogramming of fibroblasts into a pluripotent ES-cell like state. Nature 2007;448:318–324. [PubMed: 17554336]

Wong DJ, Liu H, Ridky TW, Cassarino D, Segal E, Chang HY. Module map of stem cell genes guides creation of epithelial cancer stem cells. Cell Stem Cell 2008;2:333–344. [PubMed: 18397753]

Zhang HS, Postigo AP, Dean DC. Active transcriptional repression by the Rb-E2F complex mediates G1 arrest triggered by p16INK4a, TGF-beta, and contact inhibition. Cell 1999;97:53–61. [PubMed: 10199402]

Zhang M, Rosen JM. Stem cells in the etiology and treatment of cancer. Curr. Opin. Genet. Dev 2006;16:60–64. [PubMed: 16377171]

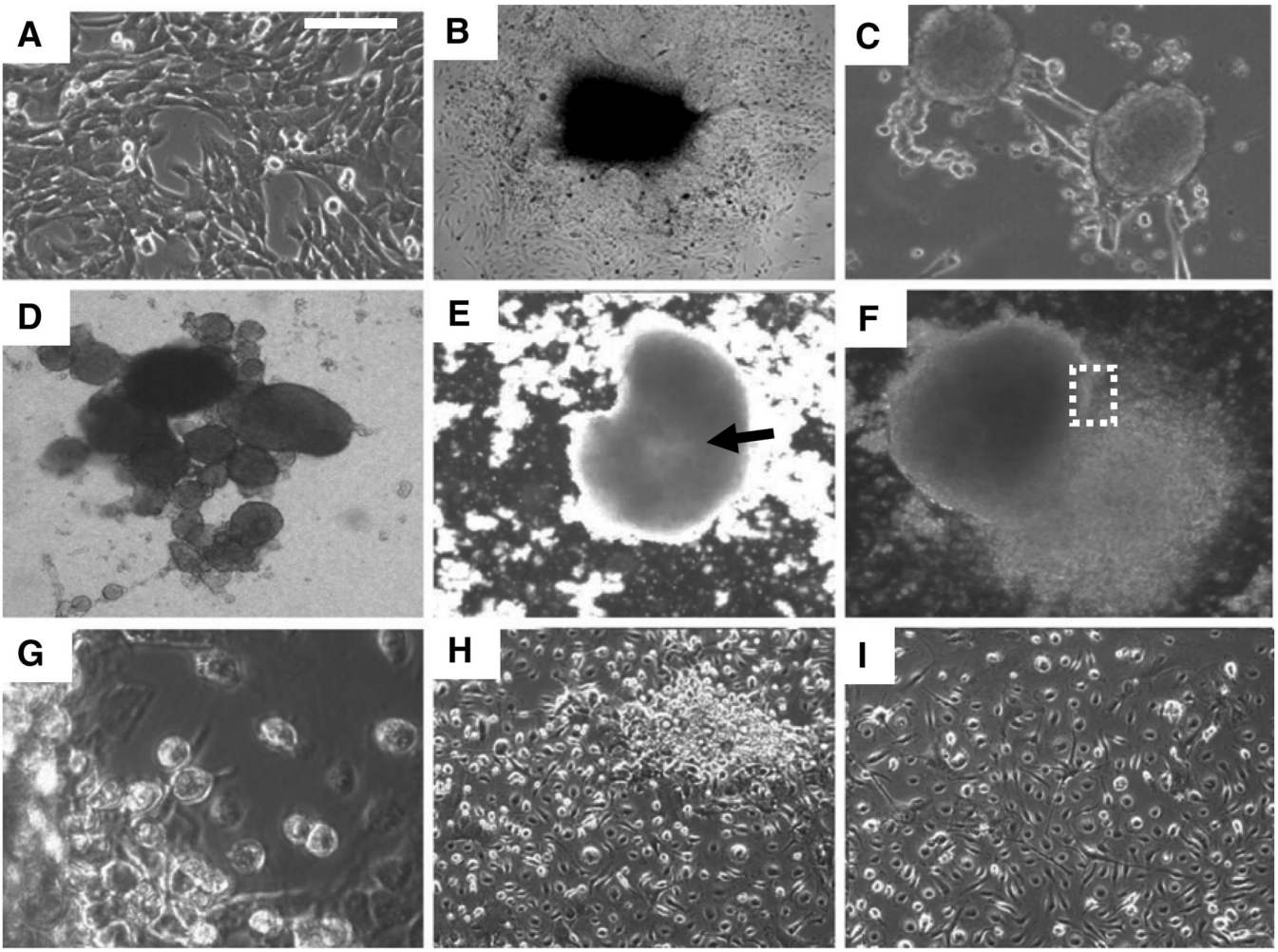

Figure 1. Sphere Formation Triggers Stable Changes in TKO Morphology

(A) TKOs at passage 4 in monolayer culture.

(B) TKOs lack contact inhibition and form mounds after reaching confluence in culture.

(C) Outgrowth of mounds, such as those shown in (B), subsequently leads to detachment from the plate and sphere formation.

(D) TKO spheres are shown 2 weeks after transfer to a nonadherent plate.

(E) Central cavity formation (arrow) becomes evident in TKO spheres after several weeks in suspension culture.

(F) TKO spheres formed in suspension culture reattached when transferred back to tissue culture plates, and all cells in the spheres migrate back onto the plate to reform a monolayer.

(G) Higher-power view of the boxed region in (F).

(H) Monolayers of sphere-derived cells 2 days after spheres were transferred back to a tissue culture plate.

(I) Cells in (H) after 1 week in culture. Note that cells in (H) and (I) have diverse morphologies, and they are smaller than TKO cells prior to sphere formation (A).

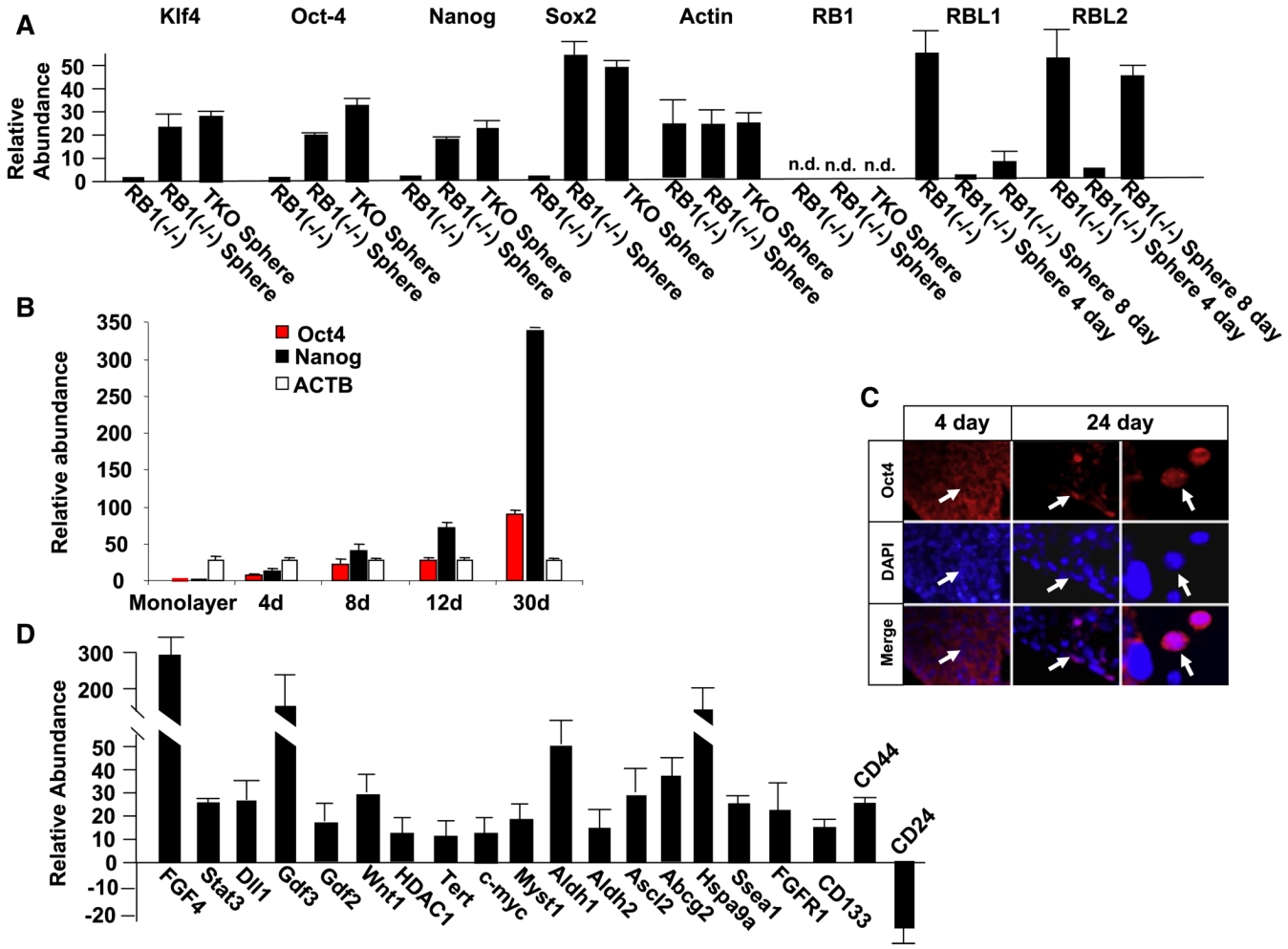

Figure 2. Sphere Formation Leads to Expression of ESC mRNAs in TKO and *RB1*$^{-/-}$ MEF Spheres, and to Downregulation of RB1 Family Members in *RB1*$^{-/-}$ MEFs

(A) Real-time PCR showing expression of mRNAs for ESC markers and RB1 family members in *RB1*$^{-/-}$ MEF spheres in suspension culture. ESC genes were analyzed after 2 weeks in suspension culture, and RB1 family members were analyzed at the indicated times.

(B) Oct-4 and Nanog mRNA increase in *RB1*$^{-/-}$ spheres with the number of days (d) in culture. Real-time PCR was used to analyze mRNA levels.

(C) Immunostaining for Oct-4 is shown in sections of *RB1*$^{-/-}$ MEFs after 4 and 24 days in culture. The right panel is a higher-power view. Note only cytoplasmic staining at 4 days, whereas nuclear staining is evident at 24 days. No staining was evident in the absence of the Oct-4 primary antibody.

(D) Real-time PCR results demonstrating changes in expression of other mRNA associated with stem cells and cancer stem cells after 2 weeks in suspension culture (also see Figures S1 and S3). The comparison is to cells in subconfluent monolayers.

Error bars indicate standard deviations.

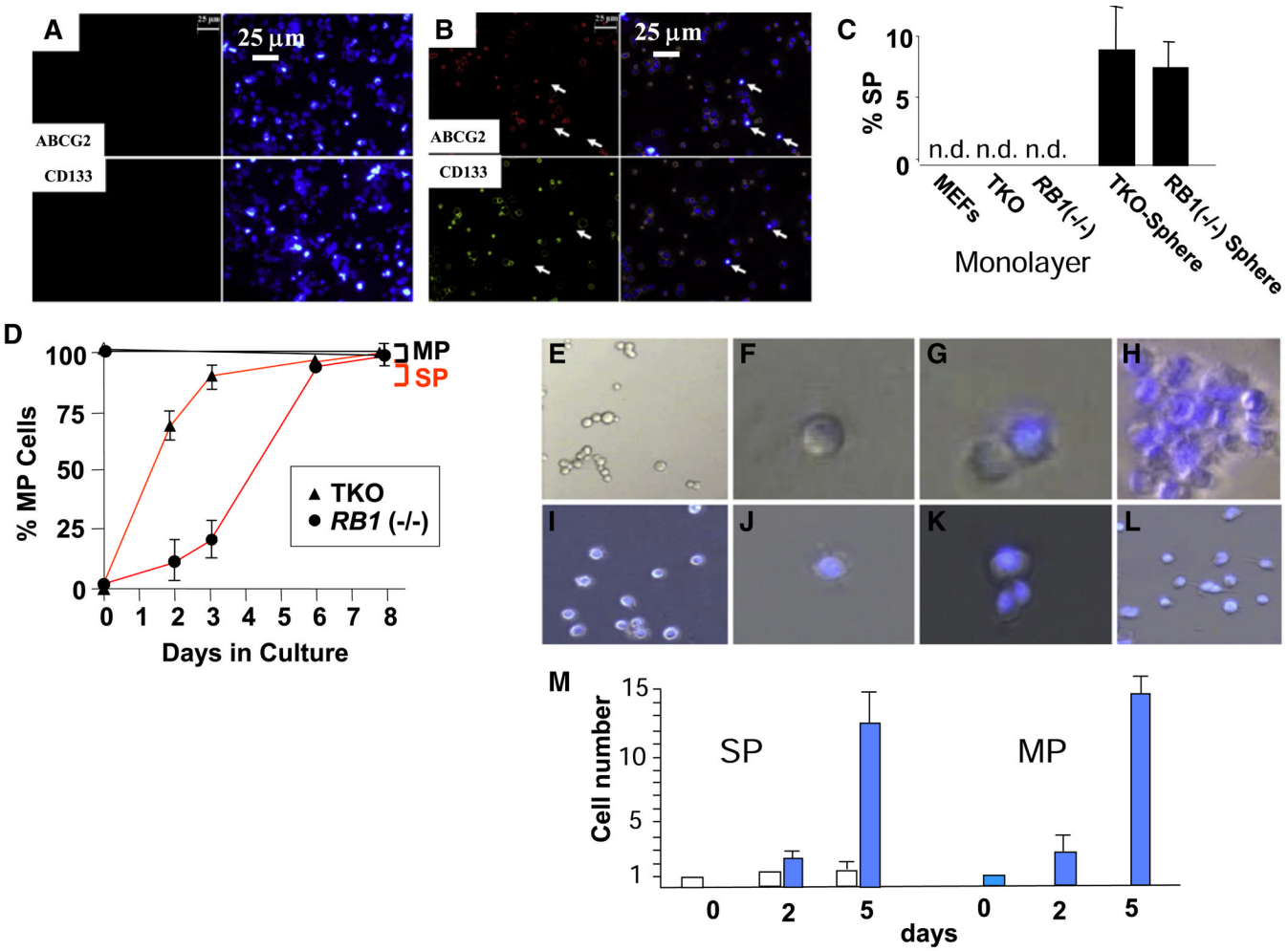

Figure 3. Sphere Formation in TKOs or *RB1*$^{-/-}$ MEFs Generates Cells with Characteristics of a Tumor SP

Immunostaining for Abcg2 and CD133 is shown on the left, and Hoechst dye staining is shown on the right.

(A) TKOs in subconfluent monolayer culture.

(B) Cells derived from TKO spheres after 2 weeks in suspension culture. Similar results were seen with cells derived from *RB1*$^{-/-}$ MEF spheres.

(C) Quantification of side population (SP) (Hoechst−, Abcg2+, CD133+) cells.

(D) TKO and *RB1*$^{-/-}$ MEF sphere-derived cells were separated into SP (Hoechst−, CD133+, Abcg2+) and MP (Hoechst+, CD133−, Abcg2−) and placed in culture (day 0). Then at the indicated times, the cells were again examined to quantify the appearance of MP cells within the SP population, and SP cells within the MP population.

(E) Hoechst− SP cells from *RB1*$^{-/-}$ MEF spheres.

(F) Higher-power view of a cell from (E).

(G) A Hoechst− cell in (E) gives rise to a Hoeschst+ cell on day 2 in culture.

(H) Population of cells arising from a single Hoechst− from (E) after 5 days in culture.

(I) Hoechst+ MP Cells.

(J) Higher-power view of a single MP cell.

(K) A Hoechst+ cell gives rise to two additional Hoeschst+ cells on day 2 in culture.

(L) Population of cells arising from a single Hoechst+ after 5 days in culture.

(M) Quantification of SP (white bars) and MP (blue bars) cells arising from single SP or MP cells. Results are from five different single SP or MP cells.
Error bars indicate standard deviations.

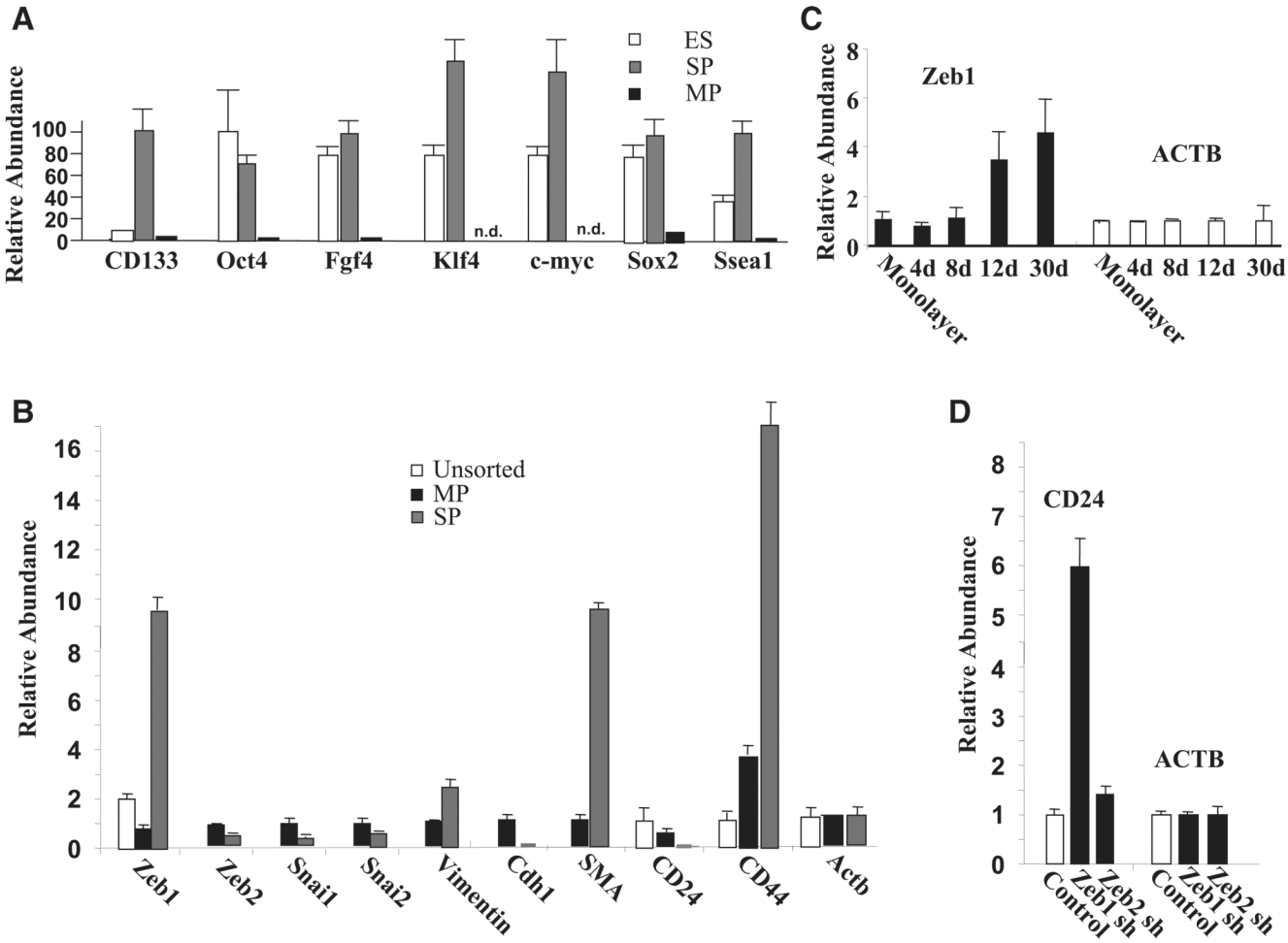

Figure 4. SP Cells Express ESC Markers, They Overexpress the EMT Transcription Factor Zeb1, and They Have a CD44-High/CD24-Low mRNA Pattern; Zeb1 Knockdown Leads to Induction of CD24 mRNA

(A) TKO sphere-derived cells were separated into SP (Hoechst−, CD133+, Abcg2+) and MP (Hoechst+, CD133−, Abcg2−) by cell sorting, and real-time PCR was used to assess the relative level of ESC mRNAs in these populations compared to ESCs maintained in monolayer culture in the presence of Lif. Results shown are normalized to β-actin (Actb) mRNA, but similar results were seen with normalization to Gapdh mRNA or β2-microglobulin mRNA (results not shown).

(B) Zeb1, but not Zeb2, Snai1, or Snai2 mRNA is induced in SP cells compared to the MP or unsorted sphere-derived cells, and this induction correlates with a CD44-high/CD24-low pattern, repression of E-cadherin (cdh1), and induction of smooth muscle actin (SMA).

(C) Zeb1 mRNA is induced in a time course during culture of *RB1*$^{-/-}$ MEFs in suspension. Real-time PCR results are shown.

(D) Knockdown of Zeb1 (Zeb1 sh) but not Zeb2 (Zeb2 sh) induces CD24 mRNA. Lentiviral shRNA constructs were used to infect MEFs and efficiently knock down Zeb1 and Zeb2 (Figure S5), and real-time PCR results are shown.

Error bars indicate standard deviations.

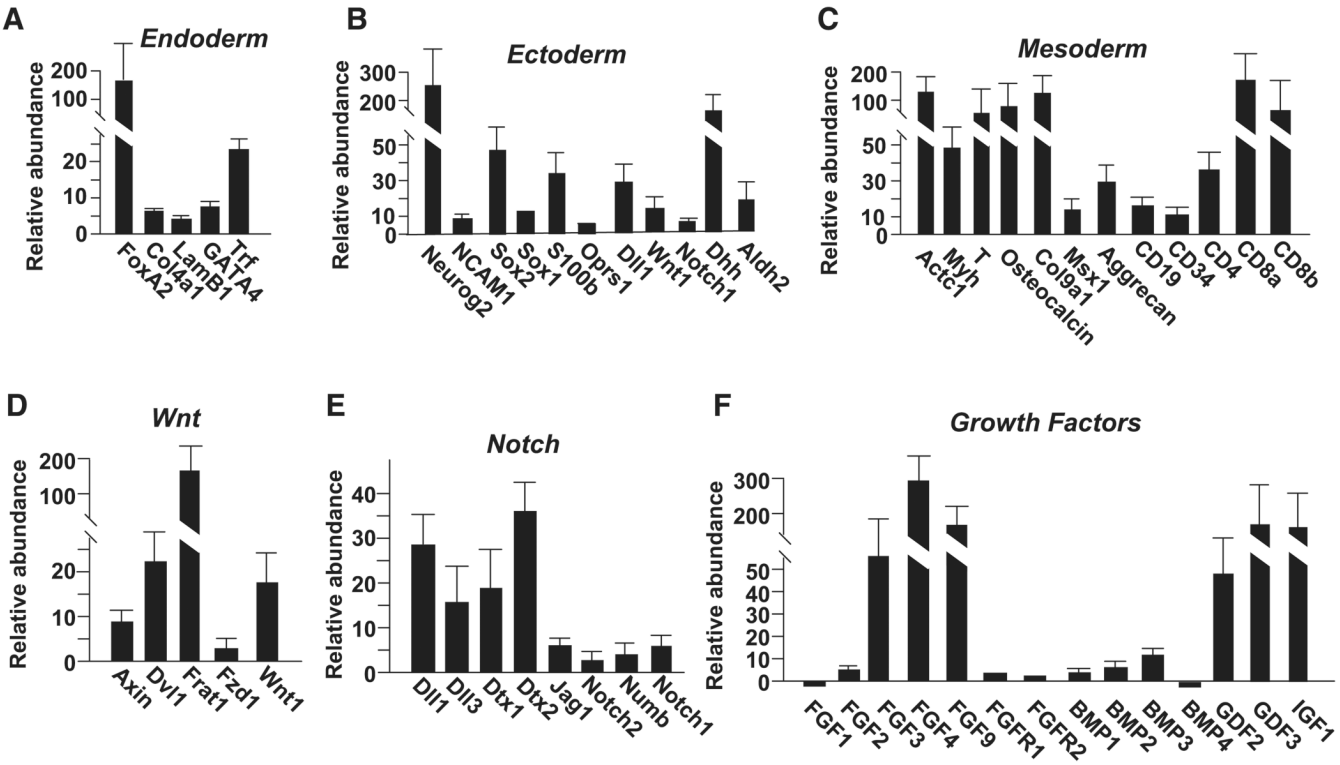

Figure 5. Sphere Formation Triggers Induction of mRNAs Representative of the Three Embryonic Layers as Well as mRNAs in Important Developmental Signaling Pathways

(A–F) Real-time PCR was used to analyze the effect of sphere formation on expression of mRNAs representative of different embryonic layers and developmental signaling pathways. Relative mRNA expression in TKO subconfluent monolayers is compared to TKO spheres that had been in suspension culture for 3 weeks. See Figures S1 and S9 for similar analysis in *RB1*$^{-/-}$ MEF spheres and cells derived from these spheres. Error bars indicate standard deviations.

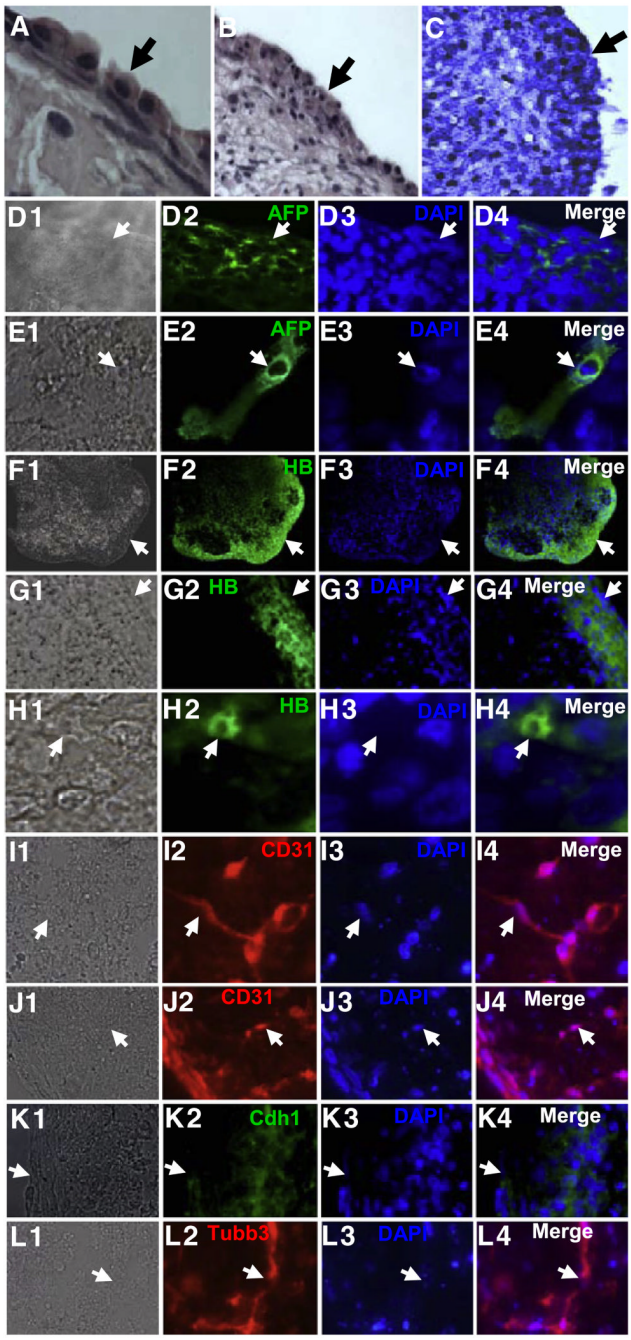

Figure 6. Immunostaining of *RB1*$^{-/-}$ Spheres Shows Expression of Markers Representative of the Three Embryonic Layers

(A) H&E-stained section showing the perimeter of an *RB1*$^{-/-}$ MEF sphere after 2 weeks in suspension culture. Note the band of cells with endodermal morphology. An arrow denotes the edge of the sphere.

(B) H&E staining showing a lower-power view of the perimeter of the sphere in (A). Note cells with epithelial-like morphology in the interior region of the sphere.

(C) A section of the sphere in (A) and (B) was stained with benzidine/peroxide, which produces a dark blue reaction in the presence of hemoglobin.

(D–L) Immunostaining of sections of *RB1*$^{-/-}$ MEF spheres. A Nomarski image is shown on the left in each panel, followed by immunostaining, DAPI staining, and a merged image on the right. Arrows denote the same position in each panel. AFP, α fetoprotein; HB, globin; Tubb3, β III tubulin; Cdh1, E-cadherin.

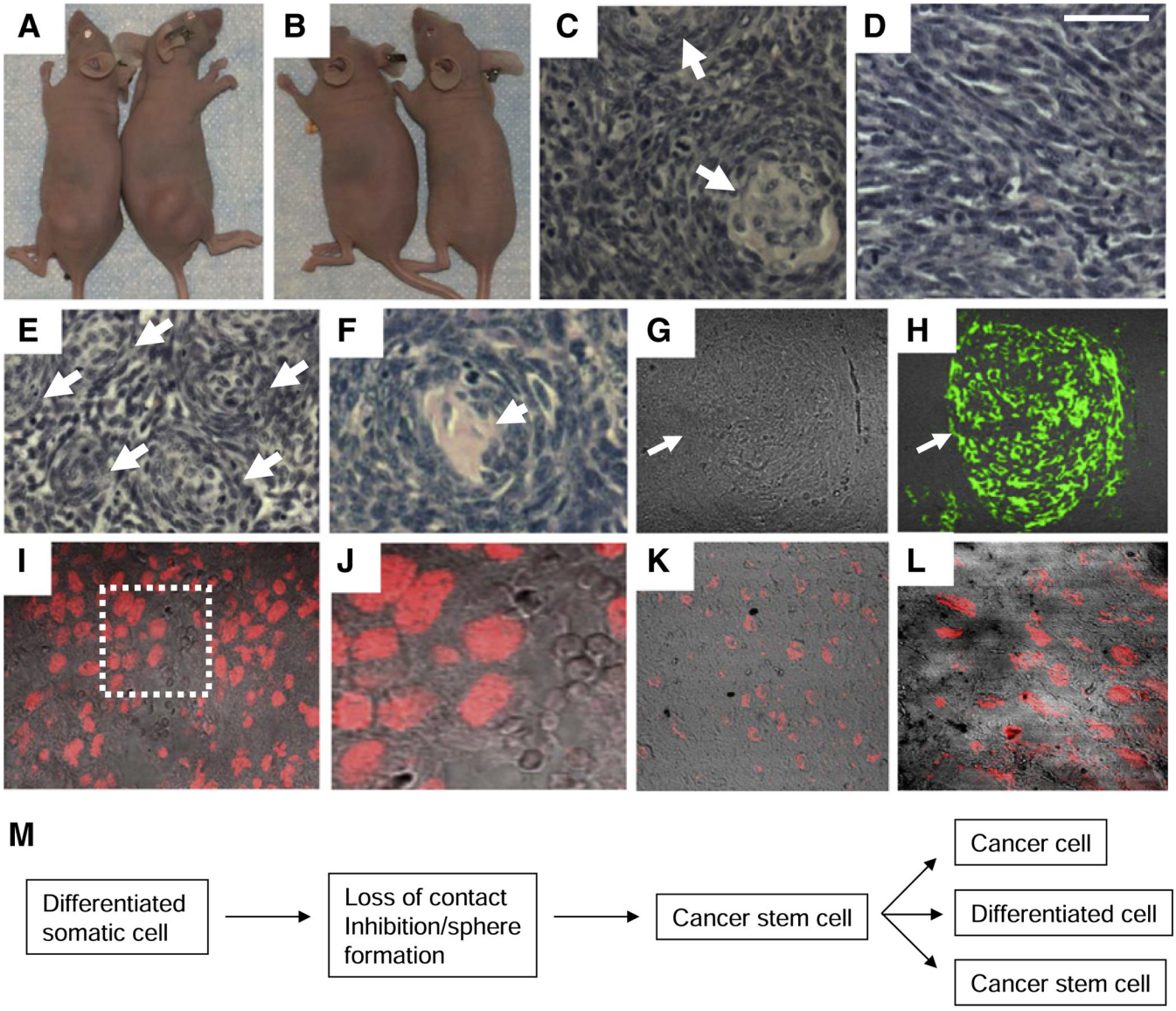

Figure 7. SP Cells Are the Primary Tumorigenic Population in the Spheres, and Tumors Derived from These Cells Consist of Cancer Cells and Neuronal Whorls

(A) Tumors formed in nude mice 3 weeks after injection of 100 SP cells subcutaneously into the hind leg.

(B) Tumors failed to form when 20,000 MP cells were injected.

(C) H&E section of a tumor formed following injection of 50,000 sphere-derived cells. Arrows indicate whorls.

(D) H&E section of a tumor formed following injection of 50,000 MP cells. Note the absence of whorls.

(E) H&E section of a tumor formed 3 weeks after injection of 100 SP cells. Note the presence of numerous closely packed whorls with eosinophilic centers (arrows).

(F) Higher-power viewofawhorl in thetumor from(E).

(G) Nomarksi image of a section of the tumor in (E).

(H) Immunostaining of the section in (G) for β III tubulin. Arrows indicate the same position in (G) and (H). Only the whorls immunostained, and tumors derived from MP cells lacked these whorls and did not immunostain.

(I and J) Nuclear immunostaining for Oct-4 in a section of an SP cell tumor. The boxed region in (I) is shown at higher power in (J).
(K and L) Nuclear immunostaining for Nanog in a section of the SP tumor. (L) is a higher-power view of the section.
(M) Model proposing a pathway for generation of cells with properties of cancer stem cells from differentiated somatic cells. See text for discussion.